Genomic Profiling and Identification of High-Risk Uveal Melanoma by Array CGH Analysis of Primary Tumors and Liver Metastases

Julien Trolet,[1,2,3] *Philippe Hupé,*[1,2,3,4] *Isabelle Huon,*[5] *Ingrid Lebigot,*[6] *Charles Decraene,*[7] *Olivier Delattre,*[8] *Xavier Sastre-Garau,*[9] *Simon Saule,*[10] *Jean-Paul Thiéry,*[7] *Corine Plancher,*[11] *Bernard Asselain,*[11] *Laurence Desjardins,*[12] *Pascale Mariani,*[13] *Sophie Piperno-Neumann,*[14] *Emmanuel Barillot,*[1,2,3] *and Jérôme Couturier*[5,8]

Purpose. Incurable metastases develop in approximately 50% of patients with uveal melanoma (UM). The purpose of this study was to analyze genomic profiles in a large series of ocular tumors and liver metastases and design a genome-based classifier for metastatic risk assessment.

Methods. A series of 86 UM tumors and 66 liver metastases were analyzed by using a BAC CGH (comparative genomic hybridization) microarray. A clustering was performed, and correlation with the metastatic status was sought among a subset of 71 patients with a minimum follow-up of 24 months. The status of chromosome 3 was further examined in the tumors, and metastases with disomy 3 were checked with an SNP microarray. A prognostic classifier was constructed using a log-linear model on minimal regions and leave-one-out cross-validation.

Results. The clustering divides the groups of tumors with disomy 3 and monosomy 3 into two and three subgroups, respectively. Same subgroups are found in primary tumors and in metastases, but with different frequencies. Isolated monosomy 3 was present in 0% of metastatic ocular tumors and in 3% of metastases. The highest metastatic rate in ocular tumors was observed in a subgroup defined by the gain of 8q with a proximal breakpoint, and losses of 3, 8p, and 16q, also most represented in metastases. A prognostic classifier that included the status of these markers led to an 85.9% classification accuracy.

Conclusions. The analysis of the status of these specific chromosome regions by genome profiling on SNP microarrays should be a reliable tool for identifying high-risk patients in future adjuvant therapy protocols. (*Invest Ophthalmol Vis Sci.* 2009;50:2572–2580) DOI:10.1167/iovs.08-2296

From the Departments of [1]Bioinformatics, [5]Genetics, [7]Translational Research, [9]Pathology, [11]Biostatistics, [12]Ophthalmology, [13]Surgery, and [14]Medical Oncology, [2]Institut National de la Santé et de la Recherche Médicale (INSERM) U900, [4]CNRS (Centre National de la Recherche Scientifique) UMR144, [6]Biological Resources Centre, [8]INSERM U830, [10]CNRS UMR146, Institut Curie, Paris, France; and [3]Ecole des Mines de Paris, ParisTech, Fontainebleau, France.

Supported by a grant from the Département de Transfert, Institut Curie, Paris, France to the Uveal Melanoma Project.

Submitted for publication May 16, 2008; revised October 31 and December 21, 2008; accepted April 9, 2009.

Disclosure: **J. Trolet**, None; **P. Hupé**, None; **I. Huon**, None; **I. Lebigot**, None; **C. Decraene**, None; **O. Delattre**, None; **X. Sastre-Garau**, None; **S. Saule**, None; **J.-P. Thiéry**, None; **C. Plancher**, None; **B. Asselain**, None; **L. Desjardins**, None; **P. Mariani**, None; **S. Piperno-Neumann**, None; **E. Barillot**, None; **J. Couturier**, None

The publication costs of this article were defrayed in part by page charge payment. This article must therefore be marked "*advertisement*" in accordance with 18 U.S.C. §1734 solely to indicate this fact.

Corresponding author: Jérôme Couturier, Department of Genetics, Institut Curie–Hôpital, 26 rue d'Ulm, F-75248 Paris Cedex 05, France; jerome.couturier@curie.net.

Uveal melanoma (UM) is the most common intraocular malignant tumor, with an incidence of approximately six cases per million per year in the Caucasian population. It shows a high propensity (in 90% of cases) to metastasize to the liver. Its prognosis is poor, with a survival of approximately 50% at 10 to 15 years, despite successful treatment of the primary tumor.[1] Ophthalmologists and oncologists have recently considered the possibility of developing adjuvant systemic treatments for high-risk patients.[2] Such treatments imply that tumors associated with a high metastatic risk at time of diagnosis can be reliable detected, to identify eligible patients. Beside clinicopathologic features (tumor size, location, histology, and extrascleral invasion), certain genomic alterations of the tumor, affecting mainly chromosomes 3, 6, and 8, have been identified by karyotype analyses, then by fluorescence in situ hybridization (FISH) and comparative genomic hybridization (CGH) (for review, see Ref. 3). The status of chromosome 3 has been shown to be strongly associated with outcome. Monosomy 3 is an early event present in 50% to 60% of tumors, often associated with the long arm of isochromosome 8, and approximately 60% of patients having a monosomic 3 tumor experience a metastatic evolution, whereas disomic 3 tumors are thought only rarely to lead metastatic disease.[4–7] In addition, other recurrent chromosome alterations, such as imbalance of chromosome 6 and losses of 1p and 16q, have been described.[8–12] Today, genome-wide techniques of genomic and expression profiling make it possible to analyze these tumors with a much higher resolution and without the limitations of cytogenetic analyses. These approaches may improve the characterization of high-risk UM. Recently, with gene expression profiling, two distinct molecular classes strongly associated with metastatic risk have been identified.[13–15] In other cancers, DNA-based techniques are known to be robust methods of classifying tumors on the basis of genomic profile. In this study, we investigated the use of array CGH for refining the identification of regions of imbalance related to metastatic evolution in UM and for the search of genes involved in the development of this tumor. To date, only two pangenomic studies of array CGH, performed on 18 and 49 primary tumors, have been reported,[16,17] and little is known about the genomic profiles of uveal melanoma metastases.[10] We report the array CGH analysis of 86 primary tumors and, for the first time, of 66 liver metastases, in an attempt to identify a genomic profile associated with high-risk UM.

Materials and Methods

Patients and Tumor Samples

Ocular tumor samples were obtained after informed consent was provided by a series of 86 unselected patients who were treated by enucleation. The study adhered to the tenets of the Declaration of Helsinki and was approved by of the Department of Translational Research and the Institutional Ethics Review Board. At first, unsupervised characterization of genome imbalances was performed on all 86 tumors. Then, for the supervised analysis regarding the metastatic

status of the patients, eight tumors of patients with a <24-month follow-up and seven tumors showing partial monosomy 3 (see the Results section) were removed, and a subset of 71 samples was used (median follow-up, 53 months; range, 24–96 months). Samples of 66 liver metastases were obtained from patients who might benefit from surgical resection. Among these samples, eight pairs of ocular tumor and the corresponding metastasis were available. All specimens included in the study were histologically confirmed and were checked on a frozen section to be certain that they contained >60% tumor cells, before DNA extraction.

Array CGH

DNA extraction, labeling, and hybridization were performed as previously described.[18] A genome-wide DNA microarray made of approximately 4 K BAC clones, FISH mapped, sequenced, verified for marker content, and spotted in triplicate, with a 1-Mb average resolution (CIT/INSERM U830, Institut Curie, Paris, France), was used. Hybridized slides were scanned (Axon GenePix 4000B scanner; Molecular Devices, Sunnyvale, CA), and image analysis was performed (Axon GenePix 5.1 software; Molecular Devices). One ocular tumor showing a minimal 3p loss in the series was analyzed on a gene microarray (250-K GeneChip; Affymetrix, Santa Clara, CA). In addition, all ocular tumors (except four samples from patients with a <2-year follow-up) and metastases showing disomy 3 (except two samples for which an adequate amount of DNA was not available) were hybridized (service provided by IntegraGen, Evry, France, on Infinium 370CNV-Quad bead; Illumina, San Diego, CA), and visualized (BeadStudio software; Illumina), to determine the allelic status of chromosome 3.

BAC Array Data Processing

Normalization. We applied the MANOR algorithm, as described by Neuvial et al.,[19] to correct for local spatial bias and continuous spatial gradient. Spots showing too low a signal-to-noise ratio or poor replicate consistency were discarded.

Alteration Detection and Minimal Regions. Each array CGH profile was centered on the median log-ratio (LR) and then analyzed by using the GLAD algorithm.[20] GLAD performs a segmentation of the genomic profile, defines regions of homogeneous DNA copy number, and returns for each of these regions a smoothing value and a status (gain, normal, or loss). For status assignment, the following thresholds were used: smoothing values ≤0.15 and >0.15 are set to loss and gain, respectively. Minimal common alterations were identified using the formalization proposed by Rouveirol et al.[21] Minimal regions supported by at least 20% of the total number of tumors of the whole dataset were considered in this analysis. Tumors were represented under three different kinds of genomic profiles: (1) The sequence of the LR values of each clone ordered along the genome (LR profile), (2) the sequence of the status of each clone (SC profile), or (3) the sequence of minimal regions (MR profile).

Clustering on Minimal Regions. Hierarchical clustering was performed on MR profiles using Euclidean distance as the similarity measure, and the Ward method to minimize the intraclass inertia during cluster building. Separation into groups was then proposed on the basis of the structure of the dendrogram.

Differential Analysis of LR Profiles. A differential analysis was performed on the LR profiles to highlight clones that have significantly different LRs between two user-defined groups of tumors. For each clone, a Student's *t*-test was performed, and the obtained probabilities were then adjusted with the Benjamini-Hochberg algorithm[22] for multiple testing correction. Clones with an adjusted $P < 10\%$ were considered to be significantly different between the two groups.

Data Visualization and Analysis. The visualization of the data, the computation of the minimal regions and clustering were performed with the VAMP software.[23]

Building of a Prognosis Classifier. Supervised classification was based on the MR profiles. Data were represented within a multiple contingency table in which each cell contained the number of tumors for the genomic category. A log-linear model was then used to analyze the contingency table and to build the classifier. The leave-one-out procedure has been used to assess the global performance, sensitivity, and specificity of the classifier. Positive and negative predictive values correspond respectively to the proportion of metastasizing primary tumors that are predicted as such and of nonmetastasizing tumors that are predicted as such. The final classifiers were computed on the whole dataset. Variable selection on the minimal regions to include in the model was performed according to Akaike's information criterion.[24] To build a classifier on continuous variables, we used a MANOVA model, and the location model was used to combine both categorical and continuous variables.[25]

Results

Genomic Profiles of Primary Ocular Tumors

Minimal regions were detected by using the whole primary ocular tumor dataset (Table 1). Partial or complete loss of chromosome 3 was found in the majority of the tumors (60/86, 70%). Among the seven tumors showing a partial loss of the chromosome, the deletions involved 3p in three cases, 3q in two cases, and both arms in two cases. The smallest region of deletion was observed in a case showing a terminal 3p loss (case T80), beyond clone RP11-34L16. The result of CGH on a gene chip (250K GeneChip; Affymetrix) showed a breakpoint at 3p25.3, between positions 8,883 800 and 8,897,506. The two deletions involving the 3q only, were large, distal to 3q11.2. Analysis (370CNV; Illumina) of the 22 cases with disomy 3 revealed one case (T22) with isodisomy 3. This case was included in the monosomy 3 group in the rest of the study. A gain involving at least the distal part of the long arm of chromosome 8, band q24, was the most frequent imbalance (77/86, 89%). On the basis of the SC profiles, the frequency of gain of individual clones of the 8q arm decreased regularly when approaching the centromere (8q11–q21.1, 52/86, 60%). Indeed, two types of 8q status were defined, whether the tumor showed an 8q gain with a proximal breakpoint (denoted hereafter as type A), located from centromere to 8q21.1, or not (type B). Type A therefore corresponded to a gain of the whole or almost the whole 8q, whereas type B was related to a gain of distal 8q or of whole chromosome 8 or to no alteration in chromosome 8. Other highly recurrent regions were also found: 6p gain (6p25-p22, 49/86, 57%), 1p loss (1p36-p12, 39/86, 45%), and 16q loss (16q23-q24, 27/86, 31%).

The hierarchical clustering (Fig. 1A), performed using the MR profiles, clearly shows, after manual verification, that chromosome 3 status defines two groups of tumors, one with disomy 3 (group 1) and the other with monosomy 3 (group 2), respectively composed of 26 and 60 cases (Table 2). Mean LR profiles were generated by computing for each clone the mean value of the LR in the tumors of a given group. The group 1 mean LR profile (Fig. 2A) showed gains of 6p and of distal 8q. The mean LR profile of group 2 (Fig. 2B) was well characterized by the loss of the whole chromosome 3 associated with the gain of the entire 8q.

The observation of the clustering dendrogram (Fig. 1A) and the minimal regions shared, led us to define two disomy 3 subgroups (1a and 1b) and three monosomy 3 subgroups (2a, 2b, and 2c; Table 2). Subgroup 1a (12 tumors) showed a 6p gain only, and subgroup 1b (14 tumors) was mainly defined by a gain of 6p associated with a loss of 6q (9/14, 64%) and by a gain of distal 8q (13/14, 93%; mean LR of 1.5). The loss of 16q appeared less often (5/14, 36%). Among the three monosomy 3 subgroups, subgroup 2a was composed of eight tumors without any minimal region other than monosomy 3. In subgroup 2b (27 tumors), monosomy 3 was associated with a relatively high-level gain of the 8q (26/27, 96%; mean LR of

TABLE 1. Status of Chromosome 3 in 86 UMs and in 66 Metastases and Presence of Metastasis in Cases with >24-Month Follow-up

Ocular Tumors				Liver Metastases		
Case	**CN 3**	**LOH 3**	**Metastasis**	**Case**	**CN 3**	**LOH 3**
T01	2×	No	No	M01	2×	No
T02	2×	No	No	M02	2×	No
T03	2×	No	No	M03	2×	No
T04	2×	No	No	M04	2×	No
T05	2×	No	Yes	M05	2×	No
T06	2×	No	Yes	M06	2×	No
T07	2×	No	No	M07	2×	No
T08	2×	No	No	M08	2×	nd
T09	2×	No	No	M09	2×	nd
T10	2×	No	No	M10	2×	Yes
T11	2×	No	No	M11	1×	—
T12	2×	No	No	M12	1×	—
T13	2×	No	No	M13	1×	—
T14	2×	No	No	M14	1×	—
T15	2×	No	Yes	M15	1×	—
T16	2×	No	No	M16	1×	—
T17	2×	No	Yes	M17	1×	—
T18	2×	No	No	M18	1×	—
T19	2×	No	No	M19	1×	—
T20	2×	No	No	M20	1×	—
T21	2×	No	No	M21	1×	—
T22	2×	Yes	Yes	M22	1×	—
T23	1×	—	No	M23	1×	—
T24	1×	—	Yes	M24	1×	—
T25	1×	—	Yes	M25	1×	—
T26	1×	—	Yes	M26	1×	—
T27	1×	—	No	M27	1×	—
T28	1×	—	No	M28	1×	—
T29	1×	—	Yes	M29	1×	—
T30	1×	—	No	M30	1×	—
T31	1×	—	No	M31	1×	—
T32	1×	—	Yes	M32	1×	—
T33	1×	—	Yes	M33	1×	—
T34	1×	—	No	M34	1×	—
T35	1×	—	Yes	M35	1×	—
T36	1×	—	Yes	M36	1×	—
T37	1×	—	Yes	M37	1×	—
T38	1×	—	Yes	M38	1×	—
T39	1×	—	Yes	M39	1×	—
T40	1×	—	No	M40	1×	—
T41	1×	—	Yes	M41	1×	—
T42	1×	—	Yes	M42	1×	—
T43	1×	—	Yes	M43	1×	—
T44	1×	—	No	M44	1×	—
T45	1×	—	Yes	M45	1×	—
T46	1×	—	Yes	M46	1×	—
T47	1×	—	Yes	M47	1×	—
T48	1×	—	Yes	M48	1×	—
T49	1×	—	Yes	M49	1×	—
T50	1×	—	Yes	M50	1×	—
T51	1×	—	Yes	M51	1×	—
T52	1×	—	Yes	M52	1×	—
T53	1×	—	No	M53	1×	—
T54	1×	—	No	M54	1×	—
T55	1×	—	Yes	M55	1×	—
T56	1×	—	No	M56	1×	—
T57	1×	—	No	M57	1×	—
T58	1×	—	Yes	M58	1×	—
T59	1×	—	No	M59	2×	LOH 3p21.31–p21.1
T60	1×	—	Yes	M60	L3p26.3	—
T61	1×	—	No	M61	L3p26.3–p26.2	—
T62	1×	—	Yes	M62	L3p26–p12	—
T63	1×	—	Yes	M63	L3p26–p12	—
T64	1×	—	Yes	M64	L3p26–p11	—
T65	1×	—	Yes	M65	L3q22–q25	—
T66	1×	—	Yes	M66	L3p26–q24	—
T67	1×	—	Yes			
T68	1×	—	Yes			

(*continues*)

TABLE 1 (*continued*). Status of Chromosome 3 in 86 UMs and in 66 Metastases and Presence of Metastasis in Cases with >24-Month Follow-up

Ocular Tumors				Liver Metastases		
Case	**CN 3**	**LOH 3**	**Metastasis**	**Case**	**CN 3**	**LOH 3**
T69	1×	—	Yes			
T70	1×	—	No			
T71	1×	—	Yes			
T72	2×	nd	<24 months			
T73	2×	nd	<24 months			
T74	2×	nd	<24 months			
T75	2×	nd	No			
T76	1×	—	<24 months			
T77	1×	—	<24 months			
T78	1×	—	<24 months			
T79	1×	—	<24 months			
T80	L3p26-p25.3	—	Yes			
T81	L3p26-p24	—	No			
T82	L3p26-p13	—	Yes			
T83	L3q12-q29	—	No			
T84	L3q11.2-q29	—	Yes			
T85	L3p26-p11, q13.3-q25	—	Yes			
T86	L3p26-p11, q26.3-q29	—	<24 months			

CN, copy number; nd, not done.

2.0), mainly of the whole arm, a loss of 8p (16/27, 59%), and a loss of 16q (11/27, 42%). Subgroup 2c (25 tumors) was characterized by a set of alterations composed of monosomy 3, a moderate gain of 8q (21/25, 84%; mean LR of 1.6), a loss of 1p (17/25, 68%), a loss of 16q (11/25, 44%), and a rare loss of 8p (6/25, 24%). Concerning the breakpoints in 8q (Table 2), most tumors of subgroup 1b belonged to type B (10/14, 71%), whereas tumors of group 2b and 2c were of type A (39/52, 75%; χ^2 test, $P = 0.0035$).

Genomic Profiles of Liver Metastases

The liver metastases dataset was processed by the same procedure, clustering analysis (Fig. 1B). Minimal regions reported pre-

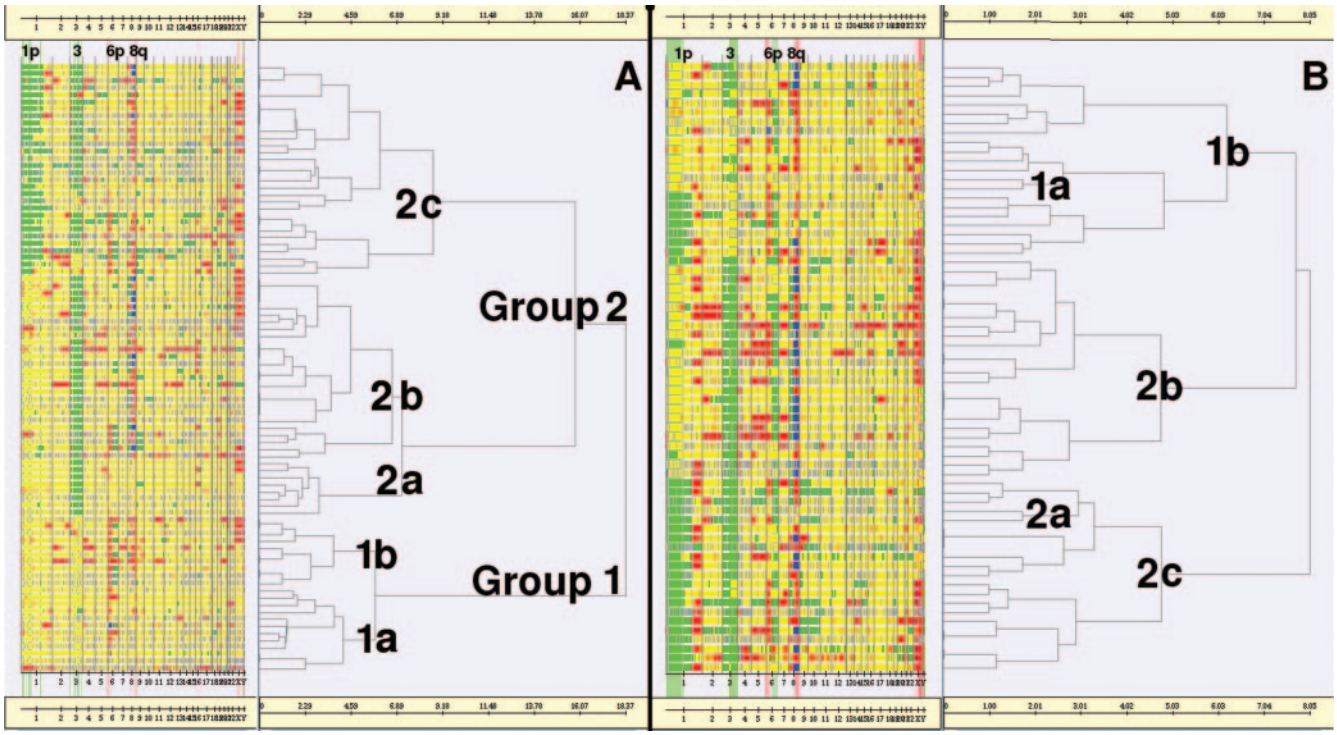

FIGURE 1. Hierarchical clustering (Ward method with Euclidean distance) of 86 ocular primary tumors (**A**) and 66 liver metastases (**B**). (**A**) Two groups of tumors (1 and 2), characterized by the status of chromosome 3, and five subgroups (1a, 1b, 2a, 2b, and 2c) can be defined on the basis of imbalances of a few chromosome regions, mainly gains of 6p and 8q and losses of 1p, 8p, and 16q. Each tumor corresponds to a row and the abscissa corresponds to the chromosomes lined up from 1 to Y. Regions gained, highly represented (LR > 3), lost, or normal, are in *red*, *blue*, *green*, and *yellow*, respectively. The dendrogram resulting from the clustering is shown on the right. (**B**) The same groups and subgroups are recognized, but with different frequencies and, on average, more altered profiles (Table 2).

TABLE 2. Tumor Subgroups in Ocular Tumors and Liver Metastases Defined from the Clustering on Seven Minimal Regions and the Rate of Metastatic Patients in the Different Subgroups of Primary Tumors

Subgroups	Imbalances	Ocular Tumors		Liver Metastasis Frequency $n = 63$
		Frequency $n = 86$	Metastasis Rate $n = 71$*	
1a	G6p	14 (12)	0 (0/10)	3 (2)
1b	G6p, L6q, G8q, L16q	16 (14)	36 (4/11)	14 (9)
2a	L3	9 (8)	0 (0/7)	3 (2)
2b	L3, L8p, G8q, L16q	31 (27)	87 (20/23)	46 (29)
2c	L1p, L3, L8p, G8q, L16q	29 (25)	75 (15/20)	33 (21)

Data are the % (*n*) of tumors in each subgroup. G, gain; L, loss.
* Sample of patients with a >24-month follow-up, after exclusion of cases with partial monosomy 3.

viously in ocular tumors were also found in liver metastases (Table 2): partial or complete monosomy 3 (48/66, 73%); gains of 8q (59/66, 89%) and 6p (21/66, 32%); and losses of 1p (31/66, 47%), 8p (30/66, 45%), and 16q (21/66, 32%). Two new frequent imbalances, gain of 1q (23/66, 35%) and loss of 6q (42/66, 64%), were observed. The mean LR of 8q gain was high (LR of 1.9). Five cases showed a partial deletion of chromosome 3 (Table 1), three in the short arm only (M62, M63, and M64), one in the long arm only (M65), and one in both arms (M66). These 3p deletions were large, with a minimal region in 3p26-p12. However, analysis of 11 metastases with disomy 3 (370CNV; Illumina) disclosed two undetected terminal deletions with breakpoints in 3p26.2 and 3p26.3 (M60 and M61). The minimal deletion was distal to SNP rs1672746 (3201 378 Mb). In addition, one case showed an isodisomy of the whole chromosome 3 (M10) and another case an interstitial LOH (loss of heterozygosity) in 3p21.3-p21.1 (9051 836 Mb), without copy number change (M59), increasing to 79% the proportion of cases with partial or complete monosomy 3.

Except for three samples showing numerous imbalances that could not be classified, liver metastases were separated into the same groups and subgroups as defined in ocular tumors (Table 2), but with different frequencies. The 11 disomy 3 samples were composed of subgroups 1a (2/11, 18%) and, predominantly, 1b (9/11, 82%). When cases with partial deletions or interstitial LOH in chromosome 3 were excluded, the 49 samples with monosomy or isodisomy 3 were distrib-

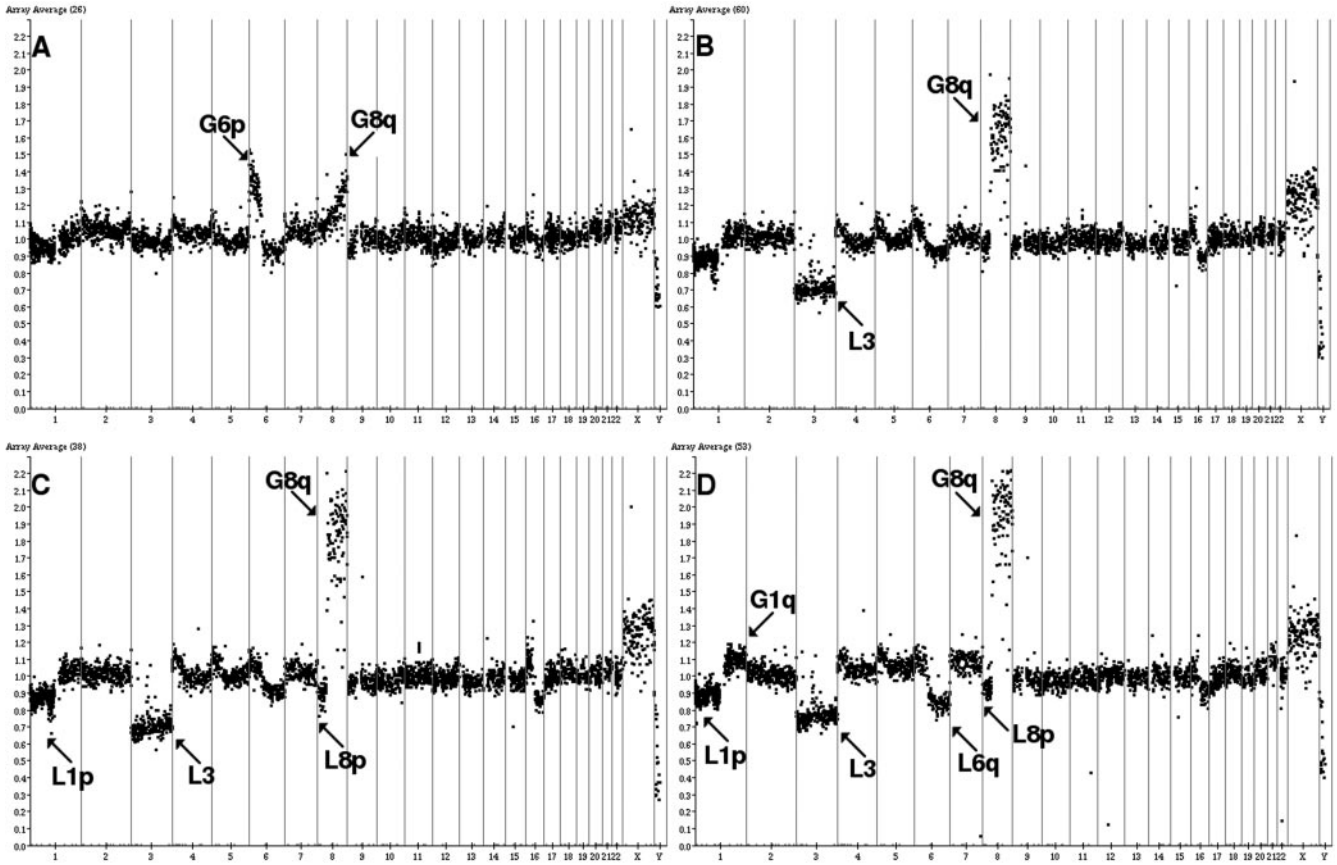

FIGURE 2. Mean LR profiles of the 26 ocular disomy 3 tumors (**A**), the 60 monosomy 3 tumors (**B**), the 38 monosomy 3 metastasizing ocular tumors (**C**), and the 53 monosomy 3 liver metastases (**D**). The abscissa corresponds to the chromosomes lined up from 1 to Y, and the ordinate is the LR between tumor and control DNAs. *Arrows*: major chromosomal alterations (G, gain; L, loss).

TABLE 3. Frequency of 8q Gains with a Proximal Breakpoint (Type A, q11.1–q21.1) in Each Subgroup of Ocular Tumors and Liver Metastases

Ocular tumors (n = 71)	
Metastatic tumors	82 (32/39)
Nonmetastatic tumors	21 (7/32)
Metastatic monosomy 3 tumors	83 (30/36)
Nonmetastatic monosomy 3 tumors	20 (3/15)
1a	0 (0/12)
1b	29 (4/14)
2a	0 (0/8)
2b	81 (22/27)
2c	68 (17/25)
Metastases (n = 63)	
1a	0 (0/2)
1b	67 (6/9)
2a	0 (0/2)
2b	93 (26/28)
2c	84 (16/19)

Data are the % (n) of tumors in each subgroup.

uted in subgroups 2a (2/49, 4%), 2b (28/49, 57%), and 2c (19/49, 39%). Thus, most of monosomy 3 metastases were assigned to subgroups 2b and 2c (49/51, 96%).

Regarding breakpoints on 8q, most of the liver metastases were of type A (50/63, 79%; Table 3).

Genomic Profiles of Paired Primary Tumors and Metastases

All these cases corresponded to group 2 tumors. Some imbalances were recurrently found as additional alterations in metastases by comparison with the corresponding ocular tumors, such as gain of 1q (3/8) and loss of 6q (3/8). One metastasis shows 11 additional copy number changes, mainly gains of whole chromosomes, in comparison with the primary tumor.

Comparison of Genomic Profiles of Ocular Tumors with Respect to Patient Metastatic Status

For this analysis, only the 71 cases without partial monosomy 3 and with a follow-up >2 years were retained. On the whole, group 2 tumors showed a higher metastatic potential (35/50, 70%) than did group 1 tumors (4/21, 19%; χ^2 test, $P = 0.0002$; Table 2). Metastasizing primary tumors significantly showed a gain of the whole 8q, with a type A breakpoint (32/39, 82%), in comparison with nonmetastasizing tumors (7/32, 22%; $P = 0.0000012$; Table 3). Among tumors with partial loss of chromosome 3, two of the three tumors with 3p loss only and one of the two with 3q loss only were associated with metastasis (Table 1). We examined separately, in monosomy and disomy 3 tumors, the eventual differences in additional chromosome imbalances according to the metastatic status of the patients.

Monosomy 3 Tumors. We compared profiles of the 35 primary tumors with full monosomy or isodisomy 3 that led to the development of liver metastases to those of the 15 nonmetastasizing ones. Metastasizing tumors predominantly showed a gain of 8q (Fig. 2C, Table 3), with a type A breakpoint (30/35, 86%), frequently associated with a loss of 8p (16/35, 46%). Conversely, nonmetastasizing tumors showed a balanced distribution of 8q breakpoints (three type A and three type B), and the loss of 8p was rare (1/15). Thus, metastasizing tumors significantly exhibited type A breakpoints (χ^2, $P = 0.0032$). In addition, metastasizing tumors showed a frequent loss of 16q (15/35, 43%), which was not frequently observed in the nonmetastatic ones (3/15, 20%). Finally, loss of 1p and gain of 6p were equally associated with nonmetastasizing (7/15, 47%, and 3/15, 20%, respectively) and with metastasizing tumors (14/35, 40%, and 7/36, 19%, respectively).

Using a differential analysis based on the LR profiles, high ratios 8p loss and 8q gain were observed in metastasizing tumors.

Disomy 3 Tumors. There were only four metastasizing monosomy three tumors in our dataset (Table 1), and they showed no specific alterations that could separate them from the 17 nonmetastasizing disomy 3 tumors.

Metastasizing Monosomy 3 Tumors Versus Monosomy 3 Metastases. Using SC profiles, frequencies of alterations were compared in the 35 monosomy 3 metastasizing ocular tumors and in the 49 monosomy 3 liver metastases. Both share the same imbalances, such as losses of 1p and 8p, and gain of whole 8q, with close frequency rates as shown on their respective mean LR profiles (Figs. 2C, 2D). However, as shown before, loss of 1p was also frequently present in nonmetastasizing tumors. Few differences existed in regions 1q and 6q which were respectively gained (21/49, 43% vs. 5/35, 14% in ocular tumors, $P = 0.01$) and lost (31/49, 63% vs 8/35, 23% in ocular tumors, $P = 0.005$) in metastases. Differential analysis showed no chromosomal regions significantly highlighted, proving that the levels of gains and losses were close in these two groups.

Determination of a High-Risk Profile in Ocular Tumors

In univariate analysis, each minimal region reported in Table 2 was assessed individually and ranked according to its predicted performance (Table 4). Monosomy 3 and gain of 8q are the most significant variables, both with 74.6% of good classification, and losses of 6p and 1p the less significant ones. Multivariate analysis, performed by adding the best remaining variables one at a time, led to better predicted performance. The best performance, 81.7% with 82.5% of specificity and 80.6% of sensitivity, was obtained with the set of the following five minimal regions: monosomy 3, gains of 6p and of 8q, and losses of 8p and 16q.

We also included the breakpoints position on 8q (types A and B) as a new categorical variable in the model, as it appeared as a characteristic feature between metastasizing and nonmetastasizing tumors. In univariate analysis, prediction performance of this new variable is better (80.3%) than any previous regions taken individually. Then, we replaced the variable gain of 8q in our previous set of five minimal regions by this new variable and improved the performance to 85.9% of good classification, with balanced specificity (89.2%) and sensitivity (82.4%), and very close positive and negative predictive values (84.6% and 87.5%). We then applied variable selection on the full model, considering all minimal regions of interest and the breakpoint position type, to remove nonsignificant variables. All variables were selected. Finally, we introduced the mean LR after breakpoint on chromosome 8q. It took the mean LR from the breakpoint on the 8q arm to the telomere, or the mean LR of the whole chromosome 8 if there was no breakpoint on the 8q. This variable was added to our best model, but performance of classification did not improve, remaining at 85.9%.

DISCUSSION

In this study, we present a genome-wide array CGH analysis performed on the largest series of UM tumors ever reported, and, for the first time, also on a series of liver metastases. In addition, a set of eight paired ocular tumors and the corresponding metastases were included.

In ocular tumors, as known for more than a decade, the most frequent imbalances are monosomy 3 and 8q gain. Among the 86 cases analyzed on BAC array, a partial chromosome 3 deletion was found in 7 cases, with a smallest region of

TABLE 4. Supervised Classification of Ocular Tumors for the Metastatic Risk

Variables	Performance of Classification	Specificity	Sensitivity	Positive Predictive Value	Negative Predictive Value
Minimal regions: univariate analysis					
L1p (p36-p12)	52.1	52.1	0.0	100.0	0.0
L6q	15.5	24.4	0.0	29.7	0.0
L16q (q23–q24)	63.4	78.3	56.2	46.2	84.4
G6p (p25-p22)	70.4	71.4	69.0	76.9	62.5
L8p (p23-p11)	67.6	94.4	58.5	43.6	96.9
L3	74.6	70.6	85.0	92.3	53.1
G8q (8q11.1-q21.1)	74.6	73.3	76.9	84.6	62.5
Minimal regions: multivariate analysis					
G8q, L3	78.9	80.0	77.4	82.1	75.0
G8q, L3, G6p	77.5	73.5	86.4	92.3	59.4
G8q, L3, L8p	80.3	80.5	80.0	84.6	75.0
G8q, L3, G6p, L8p, L16q	81.7	82.5	80.6	84.6	78.1
8q breakpoint and minimal regions					
8q breakpoint type A	80.3	82.1	78.1	82.1	78.1
L3, L8p, L16q, G6p, 8q breakpoint type A	85.9	89.2	82.4	84.6	87.5
8q log-ratio after breakpoint	73.2	83.3	65.9	64.1	84.4
L3, L8p, L16q, G6p, 8q breakpoint type A, 8q log-ratio after breakpoint	85.9	89.2	82.4	84.6	87.5

Data are percentages. Classifiers built by using a log-linear model and prediction performances assessed by using leave-one-out cross-validation. Variables used in the models are the minimal regions, 8q breakpoint position type, and 8q log-ratio after breakpoint.

deletion of 8.9 Mb, spanning 3p25.3-pter. This breakpoint, more distal than the one found by Parrella et al.,[26] matched with the proximal one of case M16397 of Tschentscher et al.,[27] which had the minimal 3p deletion in their series. However, we found by high resolution array CGH analysis two liver metastases with more distal breakpoints: in 3p26.2 and 3p26.3. In addition, one metastasis exhibited an interstitial LOH in 3p21. It should be stressed that, in addition to these microrearrangements, analysis of SNP microarrays (Illumina) enabled us to detect two cases of isodisomy 3: one in an ocular tumor and one in a liver metastasis. This anomaly has been demonstrated up to 16% of group 2 ocular tumors.[28,29]

Unsupervised clustering showed that chromosome 3 status was a stable variable that defined two groups: disomy (group 1) and monosomy 3 (group 2) tumors. Group 1 was characterized by gain of 6p as the most frequent initial imbalance. The same clustering into two main genomic groups is reported by Hughes et al.[16] and Ehlers et al.,[17] from array CGH analyses performed on 18 and 49 primary uveal melanomas, respectively. This classification is in agreement with the almost mutually exclusive relationship between monosomy 3 and gain of 6p noticed by Parella et al.[30] and Ehlers et al.[17] and their model of tumor progression. Hierarchical clustering leads to further subdivide them into subgroups based on gain of 8q, mainly, and on other highly recurrent alterations involving 1p, 8p, and 16q losses. Ehlers et al.[17] describe a third group with a normal status for chromosomes 3 and 6p and associated with the best prognosis.

The examination of 8q gains showed a discrete variation of breakpoints leading to a gain of either the whole arm or its distal part. Type A breakpoints, located close to the centromere, leading to a gain of the whole 8q, is mostly found in monosomy 3 tumors, as observed also by Hughes et al.[16] and Ehlers et al.[17] These whole 8q gains, often associated with 8p loss, are related to the presence and the frequent duplication of isochromosomes 8q, an additional abnormality well-known in karyotypic studies.[5,12,31] On the contrary, type B refers to a breakpoint distal to 8q21.1, or to an absence of breakpoint (gain of an entire chromosome 8). Most breakpoints of disomy 3 tumors belong to this type. This suggests that gains of 8q would mainly result from unbalanced translocations in group 1 and from isochromosome formation in group 2 tumors.

When genomic profiles of ocular tumors are compared with the status of the patients, group 2 tumors show a higher metastatic potential than group 1 tumors. However, of note, none of the eight tumors with isolated monosomy 3 only, (subgroup 2a) led to metastasis during the follow-up of this study (Table 2). So, early metastatic propensity appears to be only partially explained by chromosome 3 status. Indeed, subgroups with higher metastatic potential (2b, 2c, and to a lesser extent, 1b) can be identified. Contrasting with the findings of Ehlers et al.,[17] metastatic evolution appeared to be associated with 8q gain in our series, but when taking into account the position of breakpoints in 8q. Breakpoints preferentially belonged to type A, leading to whole 8q gains, in most metastasizing tumors, and to type B in nonmetastasizing ones (Table 3). Differential analysis and frequency comparison confirmed that, besides the status of chromosome 3, the main differences between metastasizing and nonmetastasizing tumors were 8q gain and 8p loss, making them high-risk indicators. This finding is in line with the recent identification of a metastatic modifier locus, *LZTS1*, in the 8p.[32] Among the six patient carriers of a tumor with partial monosomy 3, with a >24-month follow-up, four had metastases: two with a loss in 3p, one in 3q, and one in 3p and 3q. This result led us to think that genes essential for metastatic evolution are located in both arms of chromosome 3. The low number of metastasizing disomy 3 tumors prevented us from reliably comparing their profiles to those of the nonmetastasizing disomy 3 tumors.

In the liver metastases dataset, except for three samples showing highly altered profiles that could not be classified, all subgroups recognized in primary ocular tumors were found. Mostly monosomy 3 profiles (group 2) were observed, and with a higher frequency than in ocular tumors, but disomy 3 (group 1) profiles were also found (14% of the cases). Complete and partial isodisomy 3, in 3p21.31-p21.1, were disclosed by SNP (Illumina) analysis in one case each. Seven metastases showed a partial loss of chromosome 3: five of them in the 3p, with a smallest region of overlap in 3p26.3, one in the 3q, and one involving both arms. Most metastases belonged to the two monosomy 3 subgroups with a gain of 8q (2b, 2c). These gains corresponded mainly to type A breakpoints (Table 2). Two samples showed only a monosomy 3 (subgroup 2a) and two a 6p gain (subgroup

1a) as isolated imbalances, confirming that these two groups are rarely metastatic. Ten metastases (15%) belonged to subgroup 1b, which shows an intermediate metastatic rate. By comparison to ocular tumors, liver metastases specifically showed additional gain of 1q and loss of 6q in 44% and 60% of the samples, respectively. The study of the eight pairs of ocular tumors and their liver metastases showed very similar results, with a recurrent gain of 1q and a loss of 6q in metastases, in comparison with their respective primary tumor.

The classifier built in this work is designed to predict the prognosis of any individual tumor, by examining a set of a few minimal regions of interest (Table 3). In univariate analysis, gain of 8q and monosomy 3 showed better predictions for metastasizing tumors, as they presented higher positive than negative predictive values. In multivariate analysis, the best rate of classification (81.7%) was obtained when a set of five regions was combined: losses of chromosome 3, 8p, and 16q, and gain of 6p and 8q. In contrast with the observation of Kilic et al.,[33] loss of 1p, which showed a low performance of classification in univariate analysis, was not retained in the classifier. Using the 8q breakpoint position alone, we obtained 80.3% of good prediction, which was better than in univariate analysis of any of the regions. Moreover, when replacing gain of 8q by the breakpoint position in our set of five regions, we improved the classification rate to 85.9% of good classification, with balanced specificity and sensitivity, and very close positive and predictive values. Several features of our analysis suggested that the LR of 8q gain could be a pertinent prognostic indicator. First, it was apparent that high-level 8q gain was present in the subgroups of ocular tumors with the highest metastatic rates. Secondly, differential analysis result showed that monosomic metastatic tumors presented a higher 8q gain than monosomic nonmetastatic tumors. Finally, in our liver analysis of metastases, gain of 8q with a high LR was reported as the major alteration. However, although good results were obtained in univariate analysis, introducing the mean LR after breakpoint on chromosome 8q did not improved the performance of classification (85.9%).

Results from this study should provide useful information, in addition to clinicopathologic features, for designing an optimal strategy for identifying high-risk ocular tumors in a clinical setting. It has been shown that expression profiling is more sensitive and specific than genomic profiling for the prognostic evaluation of tumors,[15,34] but it is foreseeable that certain samples will yield RNA of insufficient quality for such analysis, and its applicability on individual tumors in the clinical setting remains to be determined. A DNA-based genomewide technique, including the assessment of chromosome 3 allelic status, should be an alternative tool for an optimal prognostic evaluation of UM tumors in future clinical trials.

Acknowledgments

The authors thank Sandrine Arrufat, Gaëlle Pierron, and Agnès Ribeiro, for excellent assistance in the array CGH analyses.

References

1. Diener-West M, Hauwkins BS, Markowitz JA, et al. A review of mortality from choroidal melanoma. II. A meta-analysis of 5-year mortality rates following enucleation, 1966 through 1988. *Arch Ophthalmol.* 1992;110:245–250.
2. Damato B. Developments in the management of uveal melanoma. *Clin Exp Ophthalmol.* 2004;32:639–647.
3. Mudhar HS, Parsons MA, Sisley K, et al. A critical appraisal of the prognostic and predictive factors for uveal malignant melanoma. *Histopathology.* 2004;45:1–12.
4. Prescher G, Bornfeld N, Hirche H, et al. Prognostic implications of monosomy 3 in uveal melanoma. *Lancet.* 1996;347:1222–1225.
5. Sisley K, Rennie I, Parsons M, et al. Abnormalities of chromosomes 3 and 8 in posterior uveal melanoma correlate with prognosis. *Genes Chromosomes Cancer.* 1997;19:22–28.
6. White VA, Chambers JD, Courtright PD, et al. Correlation of cytogenetic abnormalities with the outcome of patients with uveal melanoma. *Cancer.* 1998;83:354–359.
7. Damato B, Duke C, Coupland SE, et al. Cytogenetics of uveal melanoma: a 7-year clinical experience. *Ophthalmology.* 2007; 114:1925–1931.
8. Gordon K, Thompson C, Char D, et al. Comparative Genomic Hybridization in the detection of DNA copy number abnormalities in uveal melanoma. *Cancer Res.* 1994;54:4764–4768.
9. Speicher M, Prescher G, du Manoir S, et al. Chromosomal gains and losses in uveal melanomas detected by comparative genomic hybridization. *Cancer Res.* 1994;54:3817–3823.
10. Aalto Y, Eriksson L, Seregard S, et al. Concomitant loss of chromosome 3 and whole arm losses and gains of chromosome 1, 6, or 8 in metastasizing primary uveal melanoma. *Invest Ophthalmol Vis Sci.* 2001;42:313–317.
11. Sisley K, Parsons MA, Garnham J, et al. Association of specific chromosome alterations with tumour phenotype in posterior uveal melanoma. *Br J Cancer.* 2000;82:330–338.
12. Kilic E, van Gils W, Lodder E, et al. Clinical and cytogenetic analyses in uveal melanoma. *Invest Ophthalmol Vis Sci.* 2006;47: 3703–3707.
13. Tschentscher F, Husing J, Holter, et al. Tumor classification based on gene expression profiling shows that uveal melanomas with and without monosomy 3 represent two distinct entities. *Cancer Res.* 2003;63:2578–2584.
14. Onken M, Worley L, Ehlers J, et al. Gene expression profiling in uveal melanoma reveals two molecular classes and predicts metastatic death. *Cancer Res.* 2004;64:7205–7209.
15. Petrausch U, Martus P, Tönnies H, et al. Significance of gene expression analysis in uveal melanoma in comparison to standard risk factors for risk assessment of subsequent metastases. *Eye.* 2008;22(8):997–1007.
16. Hughes S, Damato BE, Giddings I, et al. Microarray comparative genomic hybridisation analysis of intraocular uveal melanomas identifies distinctive imbalances associated with loss of chromosome 3. *Br J Cancer.* 2005;93:1191–1196.
17. Ehlers JP, Worley L, Onken MD, et al. Integrative genomic analysis of aneuploidy in uveal melanoma. *Clin Cancer Res.* 2008;14:115–122.
18. Idbaih A, Marie Y, Lucchesi C, et al. BAC array CGH distinguishes mutually exclusive alterations that define clinicogenetic subtypes of gliomas. *Int J Cancer.* 2008;122:1778–1786.
19. Neuvial P, Hupé P, Brito I, et al. Spatial normalization of array-CGH data. *BMC Bioinformatics.* 2006;7:264.
20. Hupé P, Stransky N, Thiery JP, et al. Analysis of array CGH data: from signal ratio to gain and loss of DNA regions. *Bioinformatics.* 2004;20:3413–3422.
21. Rouveirol C, Stransky N, Hupé P, et al. Computation of recurrent minimal genomic alterations from array-CGH data. *Bioinformatics.* 2006;22:849–856.
22. Benjamini Y, Hochberg Y. Controlling the false discovery rate: a practical and powerful approach to multiple testing. *J R Stat Soc Series B* (*Methodological*). 1995;57:289–300.
23. La Rosa P, Viara E, Hupé P, et al. VAMP: visualization and analysis of array-CGH, transcriptome and other molecular profiles. *Bioinformatics.* 2006;22:2066–2073.
24. Sakamoto Y. Efficient use of Akaike's information criterion for model selection in high dimensional contingency table analysis. *Metron.* 1982;40:257–275.
25. Daudin JJ. Selection of variables in mixed-variable discriminant analysis. *Biometrics.* 1986;42:473–481.
26. Parrella P, Fazio VM, Gallo AP, et al. Fine mapping of chromosome 3 in uveal melanoma: identification of a minimal region of deletion on chromosomal arm 3p25.1-p25.2. *Cancer Res.* 2003;63:8507–8510.

27. Tschentscher F, Prescher G, Horsman DE, et al. Partial deletions of the long and short arm of chromosome 3 point to two tumor suppressor genes in uveal melanoma. *Cancer Res.* 2001;61:3439–3442.
28. White VA, McNeil BK, Horsman DE. Acquired homozygosity (isodisomy) of chromosome 3 in uveal melanoma. *Cancer Genet Cytogenet.* 1998;102:40–45.
29. Onken MD, Worley LA, Person E, et al. Loss of heterozygosity of chromosome 3 detected with single nucleotide polymorphisms is superior to monosomy 3 for predicting metastasis in uveal melanoma. *Clin Cancer Res.* 2007;13:2923–2927.
30. Parrella P, Sidransky D, Merbs S. Allelotype of posterior uveal melanoma: implications for a bifurcated tumor progression pathway. *Cancer Res.* 1999;59:3032–3037.
31. Prescher G, Bornfeld N, Friedrichs W, et al. Cytogenetics of twelve cases of uveal melanoma and patterns of nonrandom anomalies and isochromosome formation. *Cancer Genet Cytogenet.* 1995;80:40–46.
32. Onken MD, Worley LA, Harbour JW. A metastasis modifier locus on human chromosome 8p in uveal melanoma identified by integrative genomic analysis. *Clin Cancer Res.* 2008;14:3737–3745.
33. Kilic E, Naus C, van Gils W, et al. Concurrent loss of chromosome arm 1p and chromosome 3 predicts a decreased disease-free survival in uveal melanoma. *Invest Ophthalmol Vis Sci.* 2005;46:2253–2257.
34. Worley LA, Onken MD, Person E, et al. Transcriptomic versus chromosomal prognostic markers and clinical outcome in uveal melanoma. *Clin Cancer Res.* 2007;13:1466–1471.

E R R A T U M

Erratum in: "Control of Patterns of Corneal Innervation by Pax6" by Leiper et al. (*Invest Ophthalmol Vis Sci.* 2009;50:1122–1128.)

The listed Wellcome Trust Grant number is incorrect. The correct number is Wellcome Trust Grant 074127.